THE JOURNAL OF PHYSICAL CHEMISTRY B

Article

pubs.acs.org/JPCB

Materials Screening for the Discovery of New Half-Heuslers: Machine Learning versus ab Initio Methods

Fleur Legrain,*[,†] Jesús Carrete,[†,§] Ambroise van Roekeghem,[†] Georg K.H. Madsen,[‡] and Natalio Mingo*[,†]

[†]CEA, LITEN, 17 Rue des Martyrs, 38054 Grenoble, France

[‡]Institute of Materials Chemistry, TU Wien, A-1060 Vienna, Austria

Supporting Information

ABSTRACT: Machine learning (ML) is increasingly becoming a helpful tool in the search for novel functional compounds. Here we use classification via random forests to predict the stability of half-Heusler (HH) compounds, using only experimentally reported compounds as a training set. Cross-validation yields an excellent agreement between the fraction of compounds classified as stable and the actual fraction of truly stable compounds in the ICSD. The ML model is then employed to screen 71 178 different 1:1:1 compositions, yielding 481 likely stable candidates. The predicted stability of HH compounds from three previous high-throughput ab initio studies is critically analyzed from the perspective of the alternative ML approach. The incomplete consistency among the three separate ab initio studies and between them and the ML predictions suggest that additional factors beyond those considered by ab initio phase stability calculations might be determinant to the stability of the compounds. Such factors can include configurational entropies and quasiharmonic contributions.

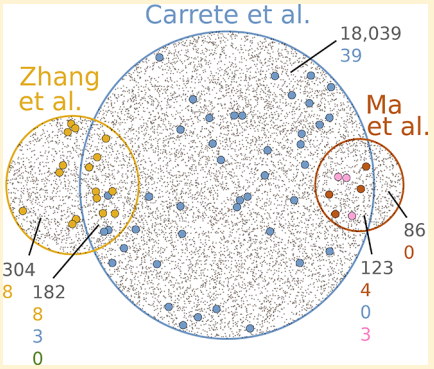

INTRODUCTION

Due to their flexible composition and resulting tunable functionalities, half-Heusler (HH) compounds are at the focus of considerable attention.[1] Substantial efforts are currently underway to discover new stable HH compounds, with successful examples in a wide range of fields including topological insulators,[2−5] magnets,[6−8] thermoelectrics,[9−12] or photovoltaics.[13] However, the large pool of possible stable HHs, in the order of thousands of compounds, is expensive to screen, both experimentally and computationally.

Several computational studies have sought to identify new stable HHs using high-throughput (HT) ab initio calculations.[8,9,14] To determine the stability of a hypothetical compound from first-principles one must test the stability of the material against all other possible phases including those that could result from the decomposition of the hypothetical compound. In addition, the enthalpies of formation should include the vibrational contributions since in many cases the stable phases at finite temperature do not correspond to the ones at 0 K.[15] This increases the cost of the already expensive calculations by orders of magnitude. Therefore, HT calculations of phase stability often neglect entropy contributions, and/or limit the number of competing phases studied.[8,9,14] The larger the number of compounds investigated, the more pressing the need for these approximations. In addition, kinetic effects are known to play an important role in the ability to synthesize a compound, and may hinder the appearance of the thermodynamically most favorable phase.[16,17] Finally, semilocal density functional theory (DFT) can have limited precision in predicting the stability of the HH compounds.[18]

A very different approach to predicting compound stability has been recently proposed in ref 19. This method uses a ML algorithm to determine the probability that a given phase is stable at a particular chemical composition. The algorithm is trained only on experimentally reported compounds, not relying on any computed formation enthalpies or ab initio data of any sort. Ref 19 applied this method to the full-Heusler compounds, demonstrating an excellent performance in cross-validation, and succeeding in predicting several stable Heusler compositions that had not been previously reported. This ML approach also has its own drawbacks, notably its reliance on the quality of the training set, and the difficulty of extracting a deeper understanding of the physics and chemistry underpinning its predictions. Nevertheless, it may prove an invaluable complement to the ab initio predictions in the search for novel compounds.

It is therefore very important to know to which extent the ML and ab initio approaches differ in their predictions, and to try to understand the possible reasons for these differences. We carry out such a comparison here. We have chosen the family of the half-Heusler compounds, because of its large number of

Special Issue: Miquel B. Salmeron Festschrift

Received: May 31, 2017
Revised: July 21, 2017
Published: July 25, 2017

DOI: 10.1021/acs.jpcb.7b05296
J. Phys. Chem. B XXXX, XXX, XXX−XXX

potential compounds, and the existence of at least three published ab initio HT studies dealing with them.[8,9,14] In what follows we first describe the pre-existing ab initio HT results, and assess their mutual consistency. Afterward we describe the ML method and our modification from its original form in order to deal with half-Heusler compounds. We then use the ML approach to screen and evaluate the stability likelihood of 71 178 half-Heuslers. Finally we compare the ML and ab initio results, and discuss the possible reasons for the differences between their predictions.

PREVIOUS AB INITIO HT STUDIES OF HALF-HEUSLER COMPOUNDS

HHs crystallize in the space group $F\bar{4}3$ M (Pearson symbol cF12) with the 1:1:1 composition (XYZ). The HH structure is shown on Figure 1. X, Y, and Z form three interpenetrating face-centered cubic sublattices, occupying 4a, 4c, and 4b Wyckoff positions, respectively. The X and Z atoms are tetrahedrally coordinated (to Y atoms) and are geometrically equivalent; interchanging them does not change the HH structure. On the other hand, the Y atom is octahedrally coordinated and it is not interchangeable with the X or Z atom without changing the structure of the material. The HH structure can be seen as XY (or YZ) forming a zincblende structure with the Z (or X) atoms filling half of the tetrahedral sites of the zincblende structure.

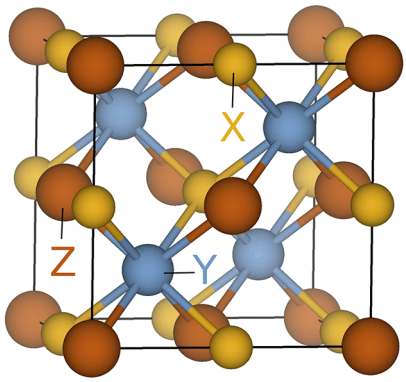

Figure 1. HH structure. X and Z sites are geometrically equivalent whereas Y site is different. A chemical composition ABC can form three different HH compounds: A, B, or C occupying the Y site.

First let us examine the consistency of the previous HT ab initio studies that explore the stability of hypothetical HH compounds, namely the works of Carrete et al.,[9] of Zhang et al.,[14] and of Ma et al.[8] The three HT ab initio studies do not employ the exact same method and do not have the exact same rules to determine the stability of the hypothetical compounds. The results of the ab initio studies are best aligned by setting the same cutoffs of formation enthalpy (0 eV) and of convex hull energy (0 eV). In this way the discrepancies pointed out in the following stem from the different methods and calculations and not from the interpretation of the results. Because the convex hull energy cutoff is set to 0 eV, only one of the three HH structures that exist per composition (see Figure 1) can be stable. Therefore, for simplicity, the comparison is performed using the composition and not each of the three structures per composition. The composition is said to be stable if the most stable HH compound out of the three possible HH structures is stable, and unstable otherwise. However, for each discrepancy, i.e., a composition stable by one study but not by the other study, it is checked that the reported stable HH structure is well explored by the other study (because of resources, the ab initio studies did not systematically consider the three possible structures).

An overview of the interrelation between the three ab initio studies is given in Figure 2. Carrete et al.,[9] Zhang et al.,[14] and

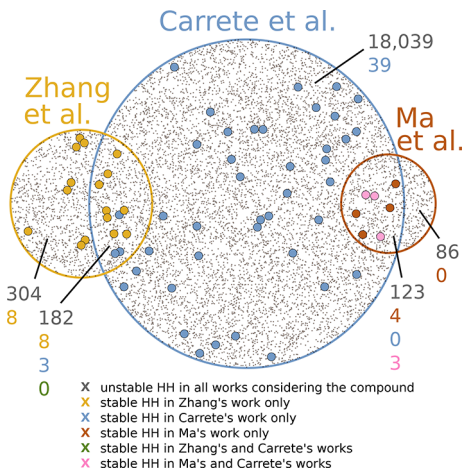

Figure 2. Points surrounded by the blue, red, and green circumferences represent the hypothetical HHs considered in Carrete's, Zhang's, and Ma's works, respectively. The intersections between the circles show the overlaps between the sets of compositions explored in the different works. The figures associated with each domain provide the number of compositions of different kinds (unstable/stable, and by which studies). The color scheme is given in the legend.

Ma et al.[8] investigated the possible stability in the HH structure of respectively 18501, 505, and 216 different compositions not already reported in the ICSD-aflow.org, either as HH or as some other prototype. As illustrated in Figure 2, 130 compositions are simultaneously contained in the studies by Carrete and by Ma, and 193 compositions are common to those by Carrete and by Zhang. There is no overlap between the sets considered by Zhang and Ma. Out of the 130 compositions common to Carrete and Ma, 7 HHs (VCoAs, MnCoAs, VRuAs, TiRhSb, TiCoAs, VCoGe, TiNiGe) are found stable by at least one of the two studies, out of which 3 (TiCoAs, VCoGe, TiNiGe) are found stable by both studies and 4 HHs (VCoAs, MnCoAs, VRuAs, TiRhSb) are found stable in Ma's work but not in Carrete's work. For the 193 compositions common to Carrete and Zhang, 3 compounds (NaSbSr, NaPCd, BaBiK) are found stable by Carrete, and 8 other (CuLiTe, AgLiTe, CuInGe, LiInSi, BeZnSi, BeZnGe, BeZnSn, ZnHgSn) are found stable by Zhang. This means that for the prediction of stable compounds there is no agreement between both works. To summarize, out of the hypothetical HHs investigated by more than one study (either by Carrete and Zhang or by Carrete and Ma), 18 are found stable by at least one study, out of which only 3 are simultaneously found stable by two studies. The remaining 15 compounds are sources of disagreement between the studies.

The origin of the discrepancies has several sources. The 3 hypothetical HHs that are found stable in Carrete's work but not in Zhang's work are due to Zhang and co-workers finding a different, more stable phase: according to Zhang's work BaBiK is more stable in the P63/mmc space group (hP6 Pearson symbol), NaPCd in the *Pnma* space group (oP12 Pearson

DOI: 10.1021/acs.jpcb.7b05296
J. Phys. Chem. B XXXX, XXX, XXX−XXX

Table 1. List of the Full Set of Descriptors with Their Relative Importance in the ML Model[a]

ranking	feature	importance
1	$\mathrm{cov}_{\mathrm{col},r}$	0.0549
2	$\mathrm{cov}_{\mathrm{col},\chi}$	0.0346
3	$\mathrm{cov}_{r,\chi}$	0.0337
4	χ_X/χ_Z	0.0283
5	$\mathrm{cov}_{\mathrm{col},m}$	0.0273
6	$\mathrm{sum}_{\mathrm{col}}$	0.0272
7	r_Z/r_Y	0.0265
8	$\chi_X - \chi_Z$	0.0262
9	$\mathrm{cov}_{Z,\mathrm{col}}$	0.0259
10	$r_Z - r_Y$	0.0247
11	r_X/r_Z	0.0236
12	m_Z	0.0235
13	χ_X	0.0230
14	$\mathrm{cov}_{\mathrm{col,row}}$	0.0227
15	Z_Z	0.0224
16	$r_X - r_Z$	0.0219
17	$\mathrm{cov}_{m,\chi}$	0.0217
18	χ_Z/χ_Y	0.0214
19	$\mathrm{cov}_{Z,m}$	0.0206
20	$\mathrm{cov}_{Z,\chi}$	0.0203
21	$\mathrm{cov}_{\mathrm{row},\chi}$	0.0197
22	χ_X/χ_Y	0.0197
23	$\mathrm{cov}_{r,m}$	0.0195
24	$\chi_Z - \chi_Y$	0.0193
25	$\mathrm{cov}_{Z,r}$	0.0188
26	$r_{\mathrm{avg(XZ)}} - r_Y$	0.0187
27	$\chi_X - \chi_Y$	0.0186
28	col_Y	0.0186
29	col_Z	0.0180
30	$\mathrm{cov}_{\mathrm{row},r}$	0.0180
31	Z_X	0.0177
32	r_Z	0.0175
33	$\mathrm{sum}_{\mathrm{col}}^{10}$	0.0171
34	r_X/r_Y	0.0170
35	$\mathrm{cov}_{\mathrm{row},m}$	0.0168
36	$r_X - r_Y$	0.0165
37	d	0.0163
38	m_X	0.0160
39	$\mathrm{cov}_{Z,\mathrm{row}}$	0.0159
40	χ_Z	0.0155
41	p	0.0152
42	r_Y	0.0149
43	χ_Y	0.0144
44	r_X	0.0140
45	Z_Y	0.0133
46	m_Y	0.0133
47	col_X	0.0122
48	row_Z	0.0048
49	row_Y	0.0043
50	s	0.0042
51	row_X	0.0037

[a]X (Z) is set as the most (least) electropositive atom. We use elemental properties of the atoms X, Y, Z (atomic number, Z; column number, col; row number, row; radius, r; mass, m; electronegativity, χ) and some of their combinations (specifically, differences and ratios of the radii and electronegativities of the different atoms). The column number of the lanthanides is set to 3. The descriptors also include the covariances between all elemental properties.[23] The covariance between two elemental properties i and j is indicated as $\mathrm{cov}_{i,j}$. Additional descriptors are the numbers of s, p, d valence electrons (s, p, d). We also consider the sum of the column numbers of the three atoms ($\mathrm{sum}_{\mathrm{col}}$), in order to account for the sum of valence electrons, as well as the modulo 10 of this sum ($\mathrm{sum}_{\mathrm{col}}^{10}$).

symbol), and NaSbSr in the *Ima*2 space group (oI36 Pearson's symbol). The inconsistencies here can be due to Zhang and co-workers correcting the DFT energies following ref 20, using DFT + U, and investigating additional competing phases (the phases were not available in the database used by ref 9 at the time, and were not explicitly included because of the computational cost.) The 8 hypothetical HHs that are found stable in Zhang's work but not in Carrete's work are so because of different reasons: Carrete's calculations gave positive formation energies for 5 HHs (CuInGe, BeZnSi, BeZnGe, BeZnSn, ZnHgSn), mechanical unstability for 1 HH (AgLiTe), and thermodynamic instability vs other competitive phases for the 2 remaining HHs (CuLiTe, LiInSi). The different signs of formation energies could be explained by the almost zero formation energies (at most at 0.11 eV from zero in the work of Zhang et al.).[21] The discrepancy in mechanical stability (AgLiTe) could also be explained by a borderline mechanical stability (a slightly distorted HH structure exists with an energy that is less than 0.15 meV/atom apart from that of the ideal HH structure).[21] The studies could give results that are on a different side of the boundary because of the different methods employed (Zhang et al. used DFT + U and added the FERE correction while Carrete et al. did not). For CuLiTe and LiInSi, Zhang et al. found them stable because they missed some intermetallic competing phases ($LiCu_3$, LiIn, $LiIn_3$) that were not available in experimental databases at the time of their calculations.[21] For the 4 hypothetical HHs that are found stable in the work of Ma but not in the work of Carrete, the reason is a mechanical unstability for 2 HHs (VCoAs, MnCoAs) and a thermodynamical unstability vs other competitive phases for the other 2 HHs (VRuAs, TiRhSb). For those last 8 + 4 HHs, the inconsistencies can be due to uncertainties in calculations (never out of the question in high-throughput studies), to approximations (in particular of not checking the mechanical stability or of not considering some competitive phases for the thermodynamical stability), or to energy discrepancies (which can sometimes be of just a few meV).

In Supporting Information an additional work from Zhang et al.[22] using ab initio high throughput to predict new stable HH compounds is compared to that of Carrete et al. and Ma et al.

MACHINE LEARNING APPROACH

We use the Scikit-learn package and employ a random forests algorithm. A random forests algorithm uses a number of trees (set to 1000 here) to make the stable/unstable classification, every tree classifying each of the inputs. Every tree is built using 6 features and no restriction is imposed on the depth of the tree. In what follows, the trees classifying the input as stable are referred as positive trees and those classifying the input as unstable as negative trees. The fractions of positive and negative trees are computed by the ML model. The classification (stable/unstable) of the input is based on the majority trees. The descriptors employed are based on the elemental properties of the three atoms of the compounds. In order to

DOI: 10.1021/acs.jpcb.7b05296
J. Phys. Chem. B XXXX, XXX, XXX−XXX

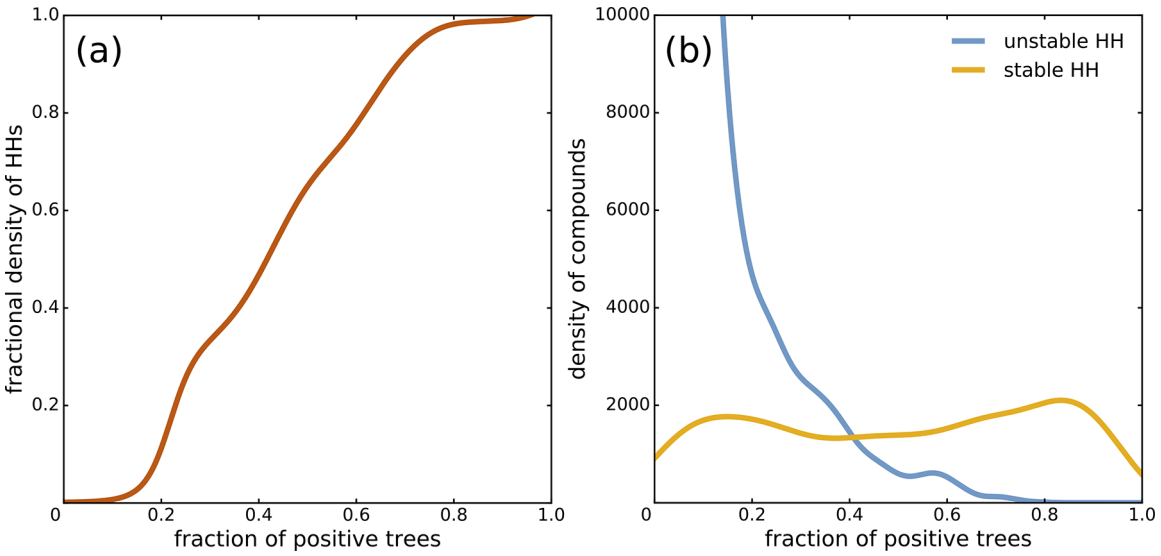

Figure 3. Plot of the outcome of the 10-fold cross-validations, i.e., for the predictions of compounds not included in the training set. The *y* axis shows the targets (the classification as listed in the ICSD-aflow.org) and the *x* axis shows the predictions (the fraction of positive trees provided by the ML model). (a) The ratio of the density of HHs over the density of all compounds ; (b) the densities of stable and unstable HHs. To plot (a) and (b), a Gaussian kernel density estimation (KDE) is used.

achieve better performance, the geometrically equivalent X and Z atoms are distinguished. Since the electronegativity of the X and Z atoms play an important role in the stability of HH,[10] X and Z are discriminated based on their electronegativities. The full list of descriptors employed is given in Table 1.

The data set employed for the training and validation consists of the compounds with the 1:1:1 (ABC) composition that are reported in the Inorganic Crystal Structure Database (ICSD) available in the aflow.org[24−26] repositories. For each 1:1:1 composition present in the ICSD-aflow.org, if one of the reported materials is a HH compound, the corresponding stable entry is added to the data set (with the correct correspondence between ABC and XYZ). If not, six unstable entries (for all possible bijections between ABC and XYZ) are added to the data set. In addition, duplicates are removed. This results in a data set of 164 stable entries and of 11 022 unstable entries.

The performance of the ML model is assessed by carrying out and averaging 10 different 10-fold cross-validations. This method evaluates the performance of the ML model on a data set not included in the training set. For the prediction of stable HHs, we obtain a precision of 0.91 (out of the 92 HHs predicted to be stable, 84 are truly stable) and a recall of 0.51 (out of the 164 truly stable HHs, 84 are predicted to be stable). The confusion matrix is provided in Supporting Information. The resulting Matthews correlation coefficient is 0.68. The performance of the ML model is evaluated differently in Figure 3a where we plot the fraction of truly stable HHs against the fraction of positive trees. The plot follows the y = x trend, showing that the fraction of positive trees really reflects the actual probability of the HHs to be stable. The ML model is therefore very helpful to guide further detailed work in the search for new stable HH compounds. Figure 3b shows the relative densities of the targets of the data set (stable/unstable) as a function of the fraction of positive trees. The plot shows that the overwhelming majority of unstable HHs are well classified (the area under the blue curve to the left of fraction of positive trees = 0.5 are the well-classified true negative). However, it also shows that part of the stable HHs are not captured by the ML model (the area under the yellow curve to the left of fraction of positive trees = 0.5 are the misclassified false negative).

Table 1 gives the relative importance of each feature. It is found that the best ranked features combine elemental properties of the different element types: the most three important features are covariances, of which the covariance between the radii and the column numbers $cov_{r,col}$ comes first. Figure 4 shows the performance of models using smaller sets of features. The features of the subsets are selected by using the recursive feature elimination method with cross-validation. The results show that the subset of 6 features allows for almost the same performance as the full set of descriptors. It contains r_Z/r_Y, χ_X/χ_Z, $cov_{col,r}$, $cov_{col,m}$, $cov_{col,\chi}$, and $cov_{r,\chi}$. The 6 features do not exactly correspond to the best 6 ranked features, due to

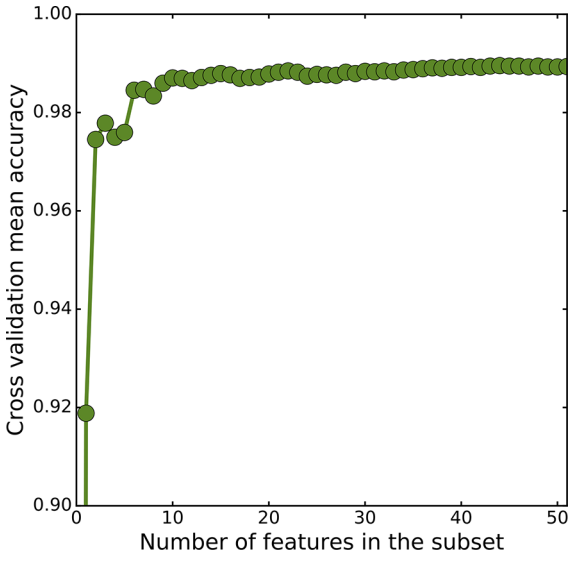

Figure 4. Plot shows the score (i.e., the mean accuracy) of subsets that results from 3-fold cross-validation against the number of selected features of the subsets. The features are selected using the recursive feature elimination method.

DOI: 10.1021/acs.jpcb.7b05296
J. Phys. Chem. B XXXX, XXX, XXX−XXX

their intercorrelation. In what follows, the full set of descriptors is used.

Screening for the Stability of 71 178 1:1:1 Compositions in the HH Structure. The ML model is used to predict the stability of 1:1:1 (ABC) compositions in the HH structure. The set of study includes all possible 1:1:1 compositions from the elements Li−Bi excluding the noble gases. The compositions already listed in the ICSD (be it in the HH structure or not) are discarded. As a result, 71 178 compositions are explored. For each composition, the 6 different bijections (between A, B, C and X, Y, Z) are considered. The results associated with the combination displaying the highest fraction of positive trees are presented. The HHs with a fraction of positive trees superior to 0.8 are given in Table 2, and all compounds with a fraction of positive trees superior to 0.5 are available in the Supporting Information. In Table 2 and in the Supporting Information, the stable HHs are given as XYZ, Y being the inequivalent atom. Although the chemical compositions listed in Table 2 and in the Supporting Information are not present in the ICSD-aflow.org repositories, and thus were absent from the training set, some of them are reported in other databases. In particular a few of them can be found in the Pauling file database.[27] Many of the hypothetical HHs predicted as most likely stable have actually already been synthesized. Furthermore, two chemical compositions, VCoGe and TiCoAs, that ab initio calculations identify to form in the HH structure but that are experimentally known to exist in another phase[18] are correctly classified by the ML model, which provide fractions of positive trees of 0.07 and 0.03 for VCoGe and TiCoAs, respectively. This lends a strong support to the predictive capabilities of the ML algorithm.

Table 2. List of the 28 Chemical Compositions with a Probability of Being HH Superior to 0.8[a]

XYZ	probability	space group
ErNiBi	0.954	216[b]
TmPtBi	0.947	216[b]
ErPdBi	0.931	216[c]
MnRuSb	0.931	
TbPtBi	0.913	216[b]
TbPdBi	0.906	216[b]
TmPdBi	0.899	216[b]
EuPdBi	0.890	
MnFeSb	0.885	227[d]
LuPtBi	0.882	216[b]
YPtBi	0.864	216[b]
EuPtBi	0.861	
TiRhSb	0.861	216[e]
ScPdBi	0.854	216[b]
MnTeRh	0.846	
HfCoBi	0.844	
LuPdBi	0.831	216[b]
MnAgSb	0.830	
TiPtSb	0.830	
TmAuPb	0.829	
VRhSb	0.827	
MnRuTe	0.822	
ZrIrBi	0.819	
MnTePt	0.819	
ScPtBi	0.813	
PmPdBi	0.812	
ZrPdBi	0.803	
MnRhSn	0.803	

[a]The "probability" is expressed as the fraction of positive trees obtained with the ML model. None of these compounds are contained in the ICSD data set we used for the training. However, many of them have been reported in the literature. In those cases the compound's space group number is provided in the third column. Space group 216 is that of the HHs. [b]Ref 28. [c]Ref 29. [d]Ref 30. [e]Ref 31.

Comparison between ab Initio Studies and ML Model Predictions. Figure 5 compares the ML predictions with those from the ab initio studies. The histograms on the bottom row of Figure 5 show the fraction of half-Heusler compounds predicted by the ab initio studies, as a function of the ML "probability", expressed as the fraction of positive trees in the random forests algorithm. The fraction of stable HHs (according to the ab initio studies) increases with the fraction of positive trees, showing some agreement between the two methods, but the agreement is not as clear as the one observed between ML and experiments (see Figure 2).

Another way of comparing the two approaches is also provided in Figure 5 (graphs at the top row). The plots show two separate curves, corresponding to the HHs and non-HHs ab initio results. The compounds within each of these two sets are ranked in order of increasing probability, and their probability (fraction of positive trees) is plotted versus this rank number. This yields two monotonically increasing curves. In the ideal case the line of the HH compounds (thick dots) should be concave, meaning that many more compounds would correspond to high ML probabilities. Similarly, the non-HH compound curve should be convex, meaning that the majority of non-HH compounds correspond to low ML probabilities. This depiction then allows for an easy visual evaluation of the agreement between ab initio and ML results.

The actual curve for the ensemble of the three studies indeed shows concave and convex shapes for the HH and non-HH sets, respectively. Looking at the separate results of each of the three ab initio studies unveils pattern differences, however. Results of Zhang et al. follow the expected concave-convex pattern quite well, meaning an agreement between the expectations from the ML classification and the actual ab initio results. Carrete's results display the expected convex pattern for the non-HH compounds, but the curve for the HHs is concave only for the higher ranked part of the data, and it has a tail of low-ranked compounds that had been nonetheless classified as HHs by the ab initio calculations. Three of the compounds in this HH tail were also classified as HHs by Ma, and two of them were given as non-HHs by Zhang. For the set of Ma et al., the HH curve is heavily weighed toward the low-probability ML values, opposite to expectation. This unexpected trend is explained by a known DFT failure. DFT calculations identify the XYAs or XYGe compounds to form in the HH structure while experimentally they exist in another structure.[18] The six HH compounds that are reported stable in Ma's work but classified as unstable by the ML model (probability inferior to 0.1) are all XYAs or XYGe compounds: VCoAs, MnCoAs, VRuAs, TiCoAs, VCoGe, and TiNiGe. Unlike DFT, ML predicts correctly the stability of those HH compounds. This reconfirms that ML methods are a great help for predicting the stability of HH compounds. The non-HH curve associated with Ma's work roughly follows the expected pattern, but there is an unexpected concave part in the 0.7−0.8 fractional rank region. These qualitative differences in shape between the three ab initio data sets may be due to the different recipes used to

DOI: 10.1021/acs.jpcb.7b05296
J. Phys. Chem. B XXXX, XXX, XXX−XXX

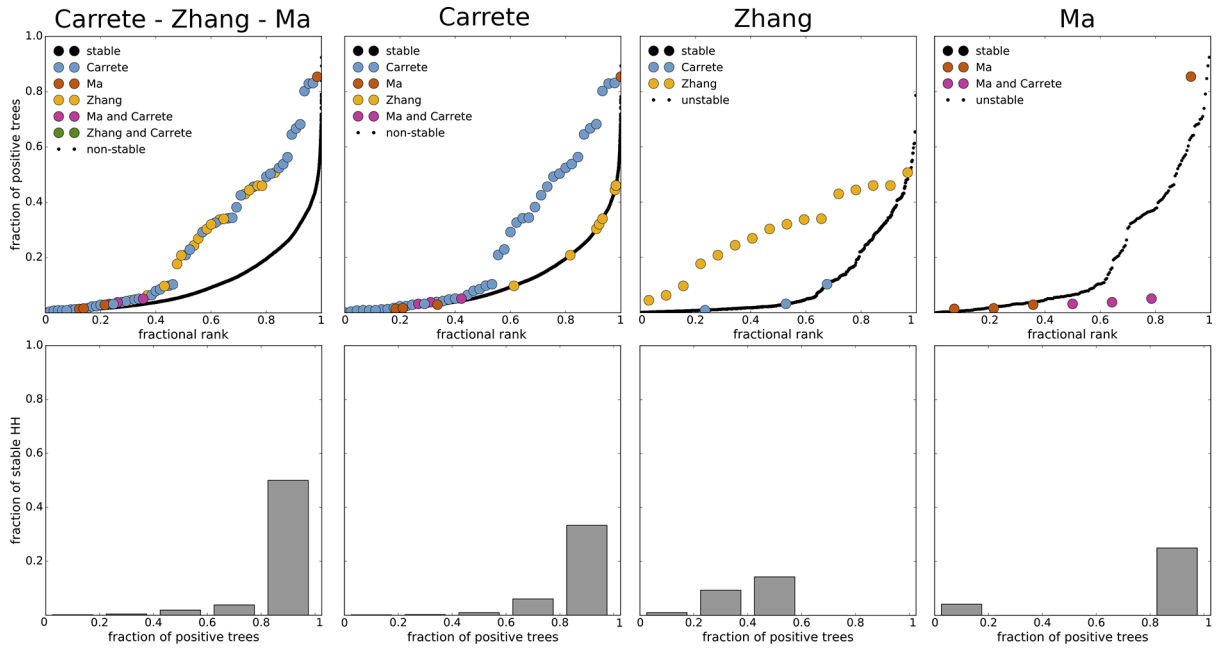

Figure 5. Comparison of the predictions from the ML model with those from the ab initio studies. The three ab initio studies (Carrete−Zhang−Ma, on the left) as well as each independent ab initio study (on the middle left, middle right, and right) are used to classify the stable/unstable HHs. For Carrete−Zhang−Ma, a HH is considered as stable if it is found stable by at least one of the three ab initio studies. Top: the *y* axis is the fraction of positive trees of the hypothetical HHs, the *x* axis represents the fractional rank of the compound in the stable and unstable lists (when the HHs are ordered in ascending order of their fraction of positive trees). Bottom: the *y* axis shows the predictions from the ab initio studies (a HH is considered as stable if it is found stable by at least one ab initio study) and the *x* axis, divided into 5 bins, shows the predictions from the ML model (more specifically the fraction of positive trees).

choose the chemical compositions of the set. Zhang's set contained compositions with 8 or 18 electron count, whereas those of Carrete and Ma were more diverse. It has also been shown that the zero-kelvin energies computed using DFT were sometimes not sufficient to correctly describe the most stable phase at standard conditions.[18] Factors such as configurational entropy and quasiharmonic contributions may also change the ordering of the free energies of competing phases.[32] When several possible configurations are competing near the ground state, entropy may stabilize the metastable solution, possibly having higher symmetry. Also, many metallic Heuslers are made through arc-melting leading to intrinsic disorder. Similar arguments have been used to discuss stabilization of other classes of materials.[16] In addition, kinetic effects may prevent formation of the thermodynamically most stable phase, in favor of a less stable one that starts nucleating earlier.[17] An alternative definition of stability based on synthesizability, taking into account the history of the material and including entropy descriptors, could be the subject of future work. Ultimately, the only way to verify the correctness of the ML and ab initio predictions is the experimental verification of the stability as given by the different methods.

CONCLUSIONS

Three different ab initio studies from the literature have provided predictions of potentially new stable HHs. Our analysis of these studies shows that, out of the 323 compositions for which the ab initio data sets overlap, 15 hypothetical HHs are found to be stable by one study but not by the other, and 3 hypothetical HHs are found to be stable by the two studies. This suggests that the methodology used today with HT ab initio methods to predict materials stability is not fully consistent among practitioners. Machine-learning algorithms are a powerful complement to ab initio methods, for they are able to guess the stable phase corresponding to a chemical composition by training the model only with experimentally reported compounds. Our ML classification of ternary compositions into half-Heusler versus nonhalf-Heusler yields an excellent performance on cross-validation, with 91% of the compounds in the HH group and over 99% of those in the non-HH group being correctly classified. It is also found that to predict the stability of a hypothetical HH, it is best to use descriptors that combine elemental properties of the different atoms. In particular the covariances between elemental properties are found to be important. We further use the algorithm to sort 71 178 previously unreported ternary compositions in order of increasing likelihood of being a stable half-Heusler, yielding a list of about 30 most likely ones worthy of further study. Some of these compositions were not listed in the ICSD used for the training, but appeared to be stable half-Heuslers in another database, confirming the reliability of the method. We have also shown that there is a certain degree of correlation between the predictions of ML and the ab initio results, with some variability among the studies. The ab initio study containing 8 and 18 electron compounds, and the lesser number of compounds, seems to be the one whose results correlate best with the ML prediction. Our results suggest that ML prediction of stable phases can represent a powerful ally of ab initio approaches for the discovery of new materials. Further work, especially in combination with experimental validation, is expected to clarify the extent and limitations of ML in this area.

ASSOCIATED CONTENT

Supporting Information

The Supporting Information is available free of charge on the ACS Publications website at DOI: 10.1021/acs.jpcb.7b05296.

DOI: 10.1021/acs.jpcb.7b05296
J. Phys. Chem. B XXXX, XXX, XXX−XXX

Chemical compositions for which the machine-learning model gives a probability to be stable in the HH structure higher than 0.5 (ZIP)

List of the HH compounds for which the ML model gives a probability of being stable that is superior to 0.5. (PDF)

AUTHOR INFORMATION

Corresponding Authors

*E-mail: fleur.legrain@cea.fr.

*E-mail: natalio.mingo@cea.fr.

ORCID

Fleur Legrain: 0000-0003-2821-8696

Jesús Carrete: 0000-0003-0971-1098

Natalio Mingo: 0000-0001-8093-0512

Present Address

§Institute of Materials Chemistry, TU Wien, A-1060 Vienna, Austria

Notes

The authors declare no competing financial interest.

ACKNOWLEDGMENTS

We thank Alex Zunger for his valuable comments and suggestions. The work is supported by M-era.net through the ICETS project (DFG: MA 5487/4-1 and ANR-14-MERA-0003-03) and ANR through the Carnot MAPPE project.

REFERENCES

(1) Casper, F.; Graf, T.; Chadov, S.; Balke, B.; Felser, C. Half-Heusler Compounds: Novel Materials for Energy and Spintronic Applications. *Semicond. Sci. Technol.* **2012**, *27*, 063001.

(2) Lin, S.-Y.; Chen, M.; Yang, X.-B.; Zhao, Y.-J.; Wu, S.-C.; Felser, C.; Yan, B. Theoretical Search for Half-Heusler Topological Insulators. *Phys. Rev. B: Condens. Matter Mater. Phys.* **2015**, *91*, 094107.

(3) Logan, J. A.; Patel, S. J.; Harrington, S. D.; Polley, C. M.; Schultz, B. D.; Balasubramanian, T.; Janotti, A.; Mikkelsen, A.; Palmstrøm, C. J. Observation of a Topologically Non-Trivial Surface State in Half-Heusler PtLuSb (001) Thin Films. *Nat. Commun.* **2016**, *7*, 11993.

(4) Nakajima, Y.; Hu, R.; Kirshenbaum, K.; Hughes, A.; Syers, P.; Wang, X.; Wang, K.; Wang, R.; Saha, S. R.; Pratt, D.; Lynn, J. W.; Paglione, J. Topological RPdBi Half-Heusler Semimetals: A New Family of Noncentrosymmetric Magnetic Superconductors. *Sci. Adv.* **2015**, *1*, e1500242.

(5) Lin, H.; Wray, L. A.; Xia, Y.; Xu, S.; Jia, S.; Cava, R. J.; Bansil, A.; Hasan, M. Z. Half-Heusler Ternary Compounds as New Multifunctional Experimental Platforms for Topological Quantum Phenomena. *Nat. Mater.* **2010**, *9*, 546−549.

(6) Felser, C.; Wollmann, L.; Chadov, S.; Fecher, G. H.; Parkin, S. S. P. Basics and Prospective of Magnetic Heusler Compounds. *APL Mater.* **2015**, *3*, 041518.

(7) Sanvito, S.; Oses, C.; Xue, J.; Tiwari, A.; Zic, M.; Archer, T.; Tozman, P.; Venkatesan, M.; Coey, M.; Curtarolo, S. Accelerated Discovery of New Magnets in the Heusler Alloy Family. *Sci. Adv.* **2017**, *3*, e1602241.

(8) Ma, J.; Hegde, V. I.; Munira, K.; Xie, Y.; Keshavarz, S.; Mildebrath, D. T.; Wolverton, C.; Ghosh, A. W.; Butler, W. H. Computational Investigation of Half-Heusler Compounds for Spintronics Applications. *Phys. Rev. B: Condens. Matter Mater. Phys.* **2017**, *95*, 024411.

(9) Carrete, J.; Li, W.; Mingo, N.; Wang, S.; Curtarolo, S. Finding Unprecedentedly Low-Thermal-Conductivity Half-Heusler Semiconductors via High-Throughput Materials Modeling. *Phys. Rev. X* **2014**, *4*, 011019.

(10) Zeier, W. G.; Schmitt, J.; Hautier, G.; Aydemir, U.; Gibbs, Z. M.; Felser, C.; Snyder, G. J. Engineering Half-Heusler Thermoelectric Materials Using Zintl Chemistry. *Nat. Rev. Mater.* **2016**, *1*, 16032.

(11) Chen, S.; Ren, Z. Recent Progress of Half-Heusler for Moderate Temperature Thermoelectric Applications. *Mater. Today* **2013**, *16*, 387−395.

(12) Zhu, T.; Fu, C.; Xie, H.; Liu, Y.; Zhao, X. High Efficiency Half-Heusler Thermoelectric Materials for Energy Harvesting. *Adv. Energy Mater.* **2015**, *5*, 1500588. 1500588.

(13) Belmiloud, N.; Boutaiba, F.; Belabbes, A.; Ferhat, M.; Bechstedt, F. Half-Heusler Compounds With a 1eV (1.7eV) Direct Band Gap, Lattice-Matched to GaAs (Si), for Solar Cell Application: A First-Principles Study. *Phys. Status Solidi B* **2016**, *253*, 889−894.

(14) Zhang, X.; Yu, L.; Zakutayev, A.; Zunger, A. Sorting Stable versus Unstable Hypothetical Compounds: The Case of Multi-Functional ABX Half-Heusler Filled Tetrahedral Structures. *Adv. Funct. Mater.* **2012**, *22*, 1425−1435.

(15) van Roekeghem, A.; Carrete, J.; Oses, C.; Curtarolo, S.; Mingo, N. High-Throughput Computation of Thermal Conductivity of High-Temperature Solid Phases: The Case of Oxide and Fluoride Perovskites. *Phys. Rev. X* **2016**, *6*, 041061.

(16) Perim, E.; Lee, D.; Liu, Y.; Toher, C.; Gong, P.; Li, Y.; Simmons, W. N.; Levy, O.; Vlassak, J. J.; Schroers, J.; Curtarolo, S. Spectral Descriptors for Bulk Metallic Glasses Based on the Thermodynamics of Competing Crystalline Phases. *Nat. Commun.* **2016**, *7*, 12315.

(17) Yong, J.; Jiang, Y.; Usanmaz, D.; Curtarolo, S.; Zhang, X.; Li, L.; Pan, X.; Shin, J.; Takeuchi, I.; Greene, R. L. Robust Topological Surface State in Kondo Insulator SmB6 Thin Films. *Appl. Phys. Lett.* **2014**, *105*, 222403.

(18) Bhattacharya, S.; Madsen, G. K. H. A Novel p-Type Half-Heusler From High-Throughput Transport and Defect Calculations. *J. Mater. Chem. C* **2016**, *4*, 11261−11268.

(19) Oliynyk, A. O.; Antono, E.; Sparks, T. D.; Ghadbeigi, L.; Gaultois, M. W.; Meredig, B.; Mar, A. High-Throughput Machine-Learning-Driven Synthesis of Full-Heusler Compounds. *Chem. Mater.* **2016**, *28*, 7324−7331.

(20) Stevanović, V.; Lany, S.; Zhang, X.; Zunger, A. Correcting Density Functional Theory For Accurate Predictions of Compound Enthalpies of Formation: Fitted Elemental-Phase Reference Energies. *Phys. Rev. B: Condens. Matter Mater. Phys.* **2012**, *85*, 115104.

(21) Zunger, A. *Private communication.*

(22) Gautier, R.; Zhang, X.; Hu, L.; Yu, L.; Lin, Y.; Sunde, T. O. L.; Chon, D.; Poeppelmeier, K. R.; Zunger, A. Prediction and Accelerated Laboratory Discovery of Previously Unknown 18-Electron ABX Compounds. *Nat. Chem.* **2015**, *7*, 308−316.

(23) Seko, A.; Hayashi, H.; Nakayama, K.; Takahashi, A.; Tanaka, I. Representation of Compounds for Machine-Learning Prediction of Physical Properties. *Phys. Rev. B: Condens. Matter Mater. Phys.* **2017**, *95*, 144110.

(24) Curtarolo, S.; Setyawan, W.; Hart, G. L.; Jahnatek, M.; Chepulskii, R. V.; Taylor, R. H.; Wang, S.; Xue, J.; Yang, K.; Levy, O.; Mehl, M. J.; Stokes, H. T.; Demchenko, D. O.; Morgan, D. AFLOW: An Automatic Framework for High-Throughput Materials Discovery. *Comput. Mater. Sci.* **2012**, *58*, 218−226.

(25) Calderon, C. E.; Plata, J. J.; Toher, C.; Oses, C.; Levy, O.; Fornari, M.; Natan, A.; Mehl, M. J.; Hart, G.; Nardelli, M. B.; Curtarolo, S. The {AFLOW} Standard for High-Throughput Materials Science Calculations. *Comput. Mater. Sci.* **2015**, *108*, 233−238.

(26) Taylor, R. H.; Rose, F.; Toher, C.; Levy, O.; Yang, K.; Nardelli, M. B.; Curtarolo, S. A {RESTful} {API} for Exchanging Materials Data in the AFLOWLIB.org Consortium. *Comput. Mater. Sci.* **2014**, *93*, 178−192.

(27) Villars, P. PAULING FILE. In *Inorganic Solid Phases*, SpringerMaterials (http://materials.springer.com/isp/crystallographic/docs/sd_1410324); Springer-Verlag: Berlin Heidelberg, 2016.

(28) Haase, M. G.; Schmidt, T.; Richter, C. G.; Block, H.; Jeitschko, W. Equiatomic Rare Earth (Ln) Transition Metal Antimonides LnTSb

DOI: 10.1021/acs.jpcb.7b05296
J. Phys. Chem. B XXXX, XXX, XXX−XXX

538 (T = Rh, lr) and Bismuthides LnTBi (T = Rh, Ni, Pd, Pt). *J. Solid State*
539 *Chem.* **2002**, *168*, 18−27.
540 (29) Sekimoto, T.; Kurosaki, K.; Muta, H.; Yamanaka, S. Thermo-
541 electric and Thermophysical Properties of ErPdX (X = Sb and Bi)
542 Half-Heusler Compounds. *J. Appl. Phys.* **2006**, *99*, 103701.
543 (30) de Groot, R.; van der Kraan, A.; Buschow, K. FeMnSb: A half-
544 metallic ferrimagnet. *J. Magn. Magn. Mater.* **1986**, *61*, 330−336.
545 (31) Dwight, A. Alloying Behavior of Zirconium, Hafnium and the
546 Actinides in Several Series of Isostructural Compounds. *J. Less-*
547 *Common Met.* **1974**, *34*, 279−284.
548 (32) Benisek, A.; Dachs, E. The vibrational and configurational
549 entropy of disordering in Cu3Au. *J. Alloys Compd.* **2015**, *632*, 585−
550 590.

DOI: 10.1021/acs.jpcb.7b05296
J. Phys. Chem. B XXXX, XXX, XXX−XXX